**Fachtagung "Experimentelle Strömungsmechanik"**
5. – 7. September 2017, Karlsruhe

# Krümmung und Torsion von Partikelbahnen innerhalb eines Modells der menschlichen leitenden Atemwege

## Curvature and torsion of particle trajectories within a model of the human conductive airways

**T. Janke, R. Schwarze, K. Bauer**
Institut für Mechanik und Fluiddynamik, TU Bergakademie Freiberg
Lampadiusstraße 4, 09599 Freiberg, Deutschland
thomas.janke@imfd.tu-freiberg.de

Krümmung, Torsion, Lungenströmung, 3D-PTV
curvature, torsion, human lung flow, 3D-PTV

### Abstract

We want to discuss the evaluation of experimental data obtained by 3D-PTV measurements, with the aim of determine local curvature and torsion values of particle trajectories. In order to achieve this, we present measurement results inside a realistic model of the human conductive airways. This transparent model reaches from the trachea down to the sixth bifurcating generation. The performed measurements correspond to realistic oscillating flow at resting conditions for an adult ($Re$ = 2000, $\alpha$ = 3.0). Our volumetric measurement setup consists of three high-speed cameras and three high-power LEDs for illumination of the measurement volume, which focuses on the area around the main carina. After covering the calculation procedure to obtain local curvature and torsion values of the measured particle trajectories we investigate the calculated curvature and torsion fields for the case of peak inspiration and peak expiration. We further evaluate single exemplary trajectories, which are strongly influenced by secondary flow effects. The results reveal the great potential of both curvature and torsion in highlighting important flow structures.

### Introduction

Flow measurements within the research field of human lung flow are often aimed at resolving the velocity field within different models and the effect of specific models on the developing secondary flows (e.g. Adler and Brücker 2007, Fresconi and Prasad 2007, Schröder *et al.* 2012, Banko *et al.* 2016). One important mechanism, which contributes towards a good mixing of air within the human airways, has been found to be the Dean-mechanism and thoroughly studied by various authors (e.g. Schroter and Sudlow 1969 , Eckmann and Grotberg 1988, Fresconi and Prasad 2007). This flow effect leads to the evolution of two counter-rotating vortices within a curved pipe flow. A mathematical solution for this problem has been presented by Dean 1928.
All previously cited experimental studies relied on measurement techniques, which represent the flow field in an Eulerian frame and no information on Lagrangian flow properties are available. In the last years, research works have been presented, which try to describe important flow characteristics by Lagrangian properties (Braun *et al.* 2006, Xu *et al.* 2007, Liberzon *et al.*

2012). With the here presented study we want to link the recent research activities of investigating the Lagrangian particle trajectory properties curvature and torsion with the research field of human lung flow.
In order to achieve this, we set up an experiment to perform three-dimensional Particle Tracking Velocimetry (3D-PTV) measurements within a model of the human airways at flow conditions similar to breathing at rest conditions ($Re$ = 2000 and $\alpha$ = 3.0). From the obtained particle paths, we derive local curvature and torsion values. After introducing the steps in order to calculate these two scalars, we present our results in two ways. At first, we show the whole reconstructed flow field and identify important areas. After that, we exemplarily illustrate two single particle paths and their corresponding curvature and torsion signals.

## Lung model and experimental set-up

The investigated lung model (see Fig. 1 a)) represents the six first bifurcation generations starting from the trachea onwards. Its geometry is generic but based on the proposed properties of a real lung by Weibel 1963 and Horsfield *et al.* 1971. A detailed overview of all its geometrical properties and about the processing steps in order to create this model is given by Adler and Brücker 2007. At this point, we just want to cover a few major characteristics. The diameter of the trachea $d_0$ is 18 mm. The two main bronchi bifurcate asymmetrically as well as all following generations. The material of the model is a transparent silicone (Elastosil RT 601) with a refractive index of $n$ = 1.4095.
To take advantage of refractive index matching techniques we are using a water-glycerin mixture (43:57 mass ratio) as the working fluid. Its dynamic viscosity is $\nu = 8.4 \cdot 10^{-6}$ Pa·s and its density is equal to $\rho$ = 1,150 kg/m$^3$. In order to perform Particle Tracking Velocimetry measurements the liquid is seeded with neutrally buoyant particles ($d_p$ = 100 µm, Vestosint).
To mimic physiologically realistic flow conditions, we generate a sinusoidal flow through the model using a linear motor (MOOG, G400 series) and diaphragm piston pump. The adjusted tidal volume of $V$ = 500 ml and the frequency of $f$ = 0.15 Hz corresponds to breathing under rest conditions at $Re$ = 2000 and $\alpha$ = 3.0.
Three high-speed cameras (Phantom v12.1, Vision Research) are used to record particle images from three different perspectives. Volumetric illumination is achieved by pulsing three high-power LEDs (PT-121, Luminus Devices) at pulse-widths of 450 µs. The image acquisition rate is set to 500 Hz. A photograph of the whole set up is presented in Fig. 1 b).

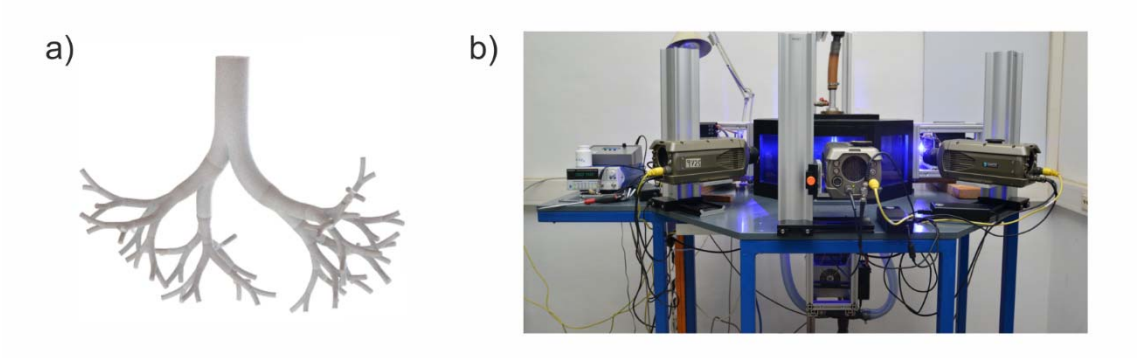


**Fig. 1** a) CAD model of the investigated lung geometry b) Photography of the experimental set-up used in this study.

## Three-dimensional Particle Tracking Velocimetry

The acquired images are evaluated using a self-developed 3D-PTV algorithm, which has already been presented by Janke and Bauer 2016. The reconstruction of the particles is done by photogrammetric methods proposed by Mass *et al.* 1993. In addition, a stepwise particle reconstruction routine has been implemented to reduce the number of occurring ghost particles. The underlying principle of such a procedure has been introduced by Wieneke 2013. The particle tracking itself is performed in two steps. At first the trajectories are initialized using a four-frame approach (Malik and Papantoniou 1993). After successfully identifying single particle paths, the further tracking is done by extrapolating the current particle position to predict its position at the next time step. If there is a matching particle in the vicinity of the predicted position, the new coordinates are adjusted accordingly, elsewise the particle is lost. This approach is based on the procedure presented by Schanz *et al.* 2013.

## Calculation of Curvature and Torsion

Starting from the results, obtained by the 3D-PTV measurements, which are typically a list of all tracked trajectories with their corresponding particle coordinates at each time step, we can calculate the local curvature $\kappa$ and torsion $\tau$ along the particle path. Curvature and torsion are two scalars, which characterize the geometry of a space curve. Whereat the curvature is a measure of how strong a particle path differs from a straight line and the torsion gives a measure for how strong the curve bends away from the plane of curvature. With the following definitions these two scalars can be calculated:

$$\boldsymbol{\kappa} = \frac{\left|\underline{\dot{x}} \times \underline{\ddot{x}}\right|}{\left|\underline{\dot{x}}\right|^3} \tag{1}$$

$$\boldsymbol{\tau} = \frac{\underline{\dot{x}} \cdot (\underline{\ddot{x}} \times \underline{\dddot{x}})}{|\underline{\dot{x}} \times \underline{\ddot{x}}|^2} \tag{2}$$

In these equations $\underline{x}$ denotes the time dependent world-coordinates of the curve or particle position in our case. The number of dots above $\underline{x}$ indicates the order of the time derivation. To provide a better understanding of the curvature and torsion, we want to discuss both quantities in a simple example – a helix-curve with a constant radius *r* and a constant rise *a* (see Fig. 2). The coordinates of such a curve can be described as followed:

$$\boldsymbol{x(t)} = \boldsymbol{r \cdot \sin(t)} \tag{3}$$

$$\boldsymbol{y(t)} = \boldsymbol{r \cdot cos(t)} \tag{4}$$

$$\boldsymbol{z(t)} = \boldsymbol{a \cdot t} \tag{5}$$

To cover a full turn of the curve, we want to define *t* in the range between $t = 0 \ldots 2\pi$. With values of $r = 1$ and $a = 1$, we obtain the space-curve illustrated in Fig. 2. With equations (1) and (2) we can calculate the curvature and torsion for this case as $\kappa = 0.5$ and $\tau = 0.5$. Since our PTV results represent discrete points of a particle path, both the curvature and torsion can only be evaluated at those discrete points. Therefore all needed time derivatives have to be formulated in a discrete manner and are calculated by a central differencing scheme for our case. The problem with such numerical derivatives is, that they are highly affected by any occurring noise in the data, especially for the case when there is a need for higher derivatives, like the third time derivative for the calculation of the torsion.


Karlsruhe, Germany, ISBN 978-3-9816764-3-3

To show the influence of this effect, we discretize the previously defined helix-curve with one hundred data points and added a random noise with a standard deviation of $\sigma$ = 0.001. The calculated curvature and torsion values are plotted in Fig. 2. As we can see, there are fluctuations within both signals, which are not physically but a consequence of the numerical calculation. Using a robust smoothing algorithm (Garcia 2010), we are still able to recover the mean values.

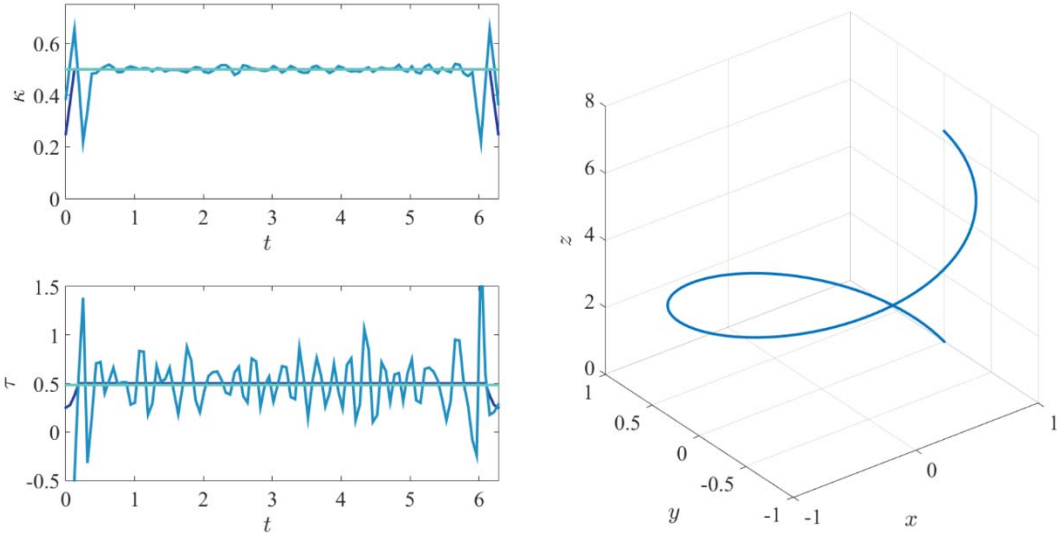


**Fig. 2** Values of curvature $\kappa$ and torsion $\tau$ (left; signal of ground truth, signal of noisy data, smoothed data) along a helical space-curve with constant radius and rise (right).

## Results and Discussion

For the measurements, carried out here, we are able to reconstruct a total number of around 11,000 particle paths with a minimum tracked period of five time steps. For the results, shown here, only particle paths with a tracked period of at least ten time steps are evaluated in order to reduce the influence of falsely reconstructed trajectories. In Fig. 3 those particle paths are illustrated for the cases of peak inspiration and peak expiration. In addition, the trajectories are color-coded with either their calculated local curvature or torsion value. The reconstructed volume is shown in top view with the trachea in the center, the left main bronchi is located on the right side, and the right main bronchi on the left.

For the case of peak inspiration, areas of high curvature can be found at those positions, where the well-known Dean vortices start to develop. As a result, near-wall particles are forced into a helical motion towards the center line of the airway. With the corresponding torsion representation we are able to determine the sense of rotation of these helical structures. Whereat positive torsion values indicate a right-handed rotation in the direction of flow and negative torsion values a left-handed one. We can find this clear separation of counter-rotating structures down to the third generation of bifurcation.

For the flow phase at peak expiration a clear symmetry within the first bifurcation, as seen during the inspirational flow phase, cannot be found. The maximum curvature values are also slightly smaller for the case of expiration. As already stated in other studies (Adler and Brücker 2007; Fresconi and Prasad 2007; Coletti and Elkins 2015), we can detect a four vortex pattern within the trachea. But we find the posterior vortex, originating from the right primary bronchus, to result in significantly higher curvature values. The volume representation, color-coded with the torsion, is revealing the separate counter-rotating structures very well as already seen for the case of inspirational flow.

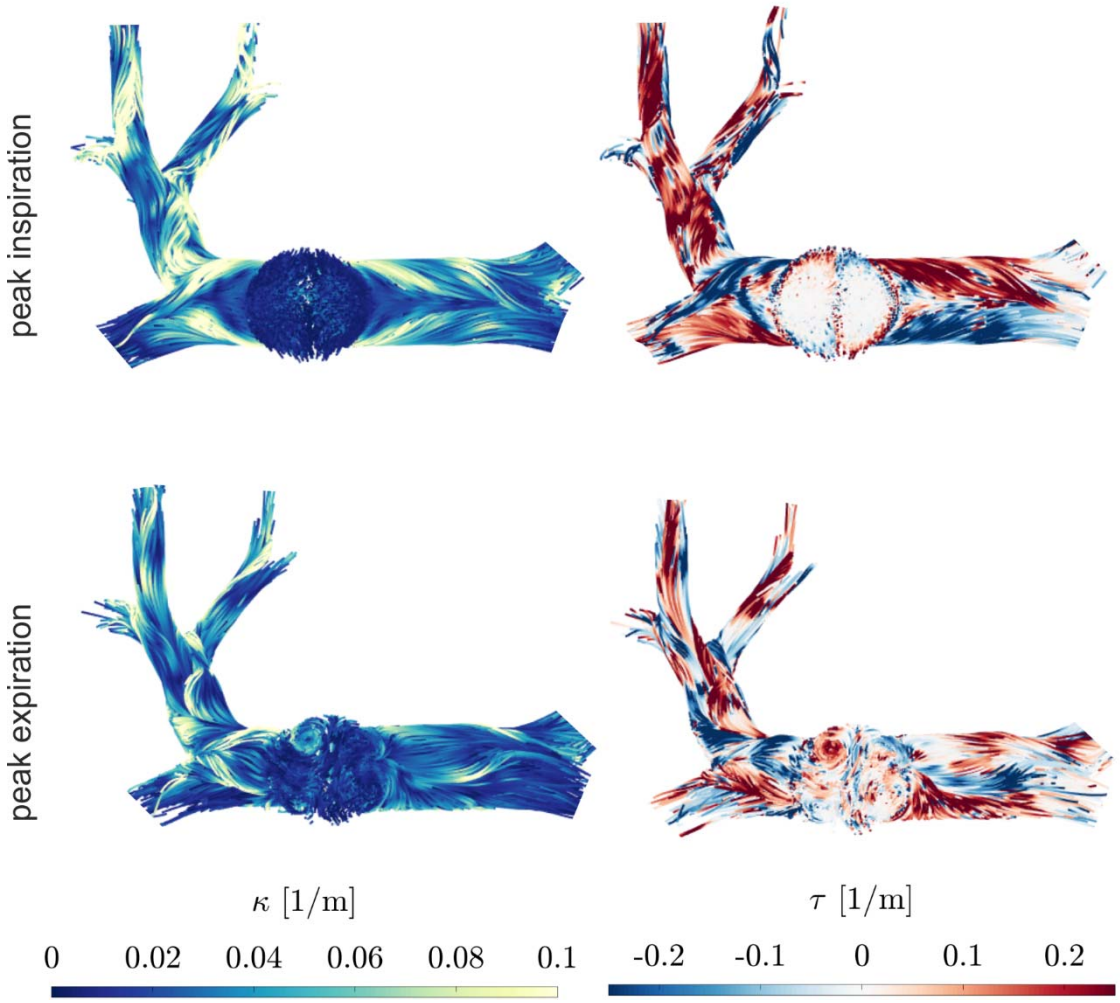


**Fig. 3** Local curvature (left) and local torsion (right) of reconstructed particle trajectories for *Re* = 2000 and *α* = 3.0 at peak inspiration (upper row) and peak expiration (lower row).

The next results we want to present are single exemplary particle trajectories for both flow phases. For each of them, we illustrate their position within the flow field, a top-down view of its path, as well as their calculated curvature and torsion signal (with and without smoothing). In Fig. 4 a particle path during peak inspiration is illustrated. The particle starts in the trachea, passes the right main bronchus and is lost after it has reached the next daughter generation. During this path, two areas with high curvature can be identified. The first one is at the main carina, where the flow is divided. The second one is right after, where the particle is under the influence of secondary flow motion, which leads to a traverse of the particle from the posterior to the anterior side of the model.

A chosen particle path for peak expiration is shown in Fig. 5. The tracked particle was detected at the first daughter bifurcation of the left main bronchus and could be tracked until it reached the tracheal area. Originating from the lower branches at a near-wall position, the particle was trapped by a vortex, resulting in a tight winding spiral motion right after the bifurcation. This spiral stretches, the further the particle travels downstream in the left bronchus until no helical motion can be detected anymore. Along this particle path four curvature maxima can be detected. The first one is linked to the change of direction, where the particle is transported from the near-wall position towards a more centered position within the airway. At position 2, the particle got trapped within a vortex, where it starts to spiral around a center axis. This is also indicated by a slowly increasing torsion value. The torsion increases, as the spiral gets

stretched and decreases again as the influence of the vortex vanishes. Positions, marked with the numbers 3 and 4 reveal, that the curvature value is not constant but reaches local maxima in a periodically manner.

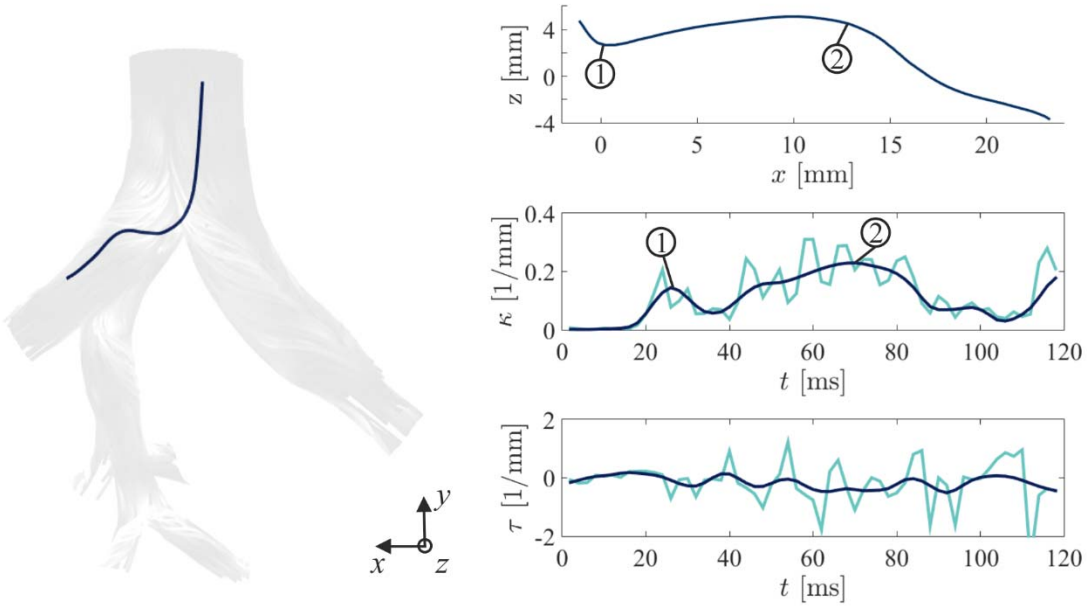


**Fig. 4** Evaluation of a single particle trajectory during peak inspiration. Illustration of the particle path position within the reconstructed volume (left), particle path in x-z-plane (right-top), curvature signal: raw, smoothed (right-middle), torsion signal: raw, smoothed (right-bottom).

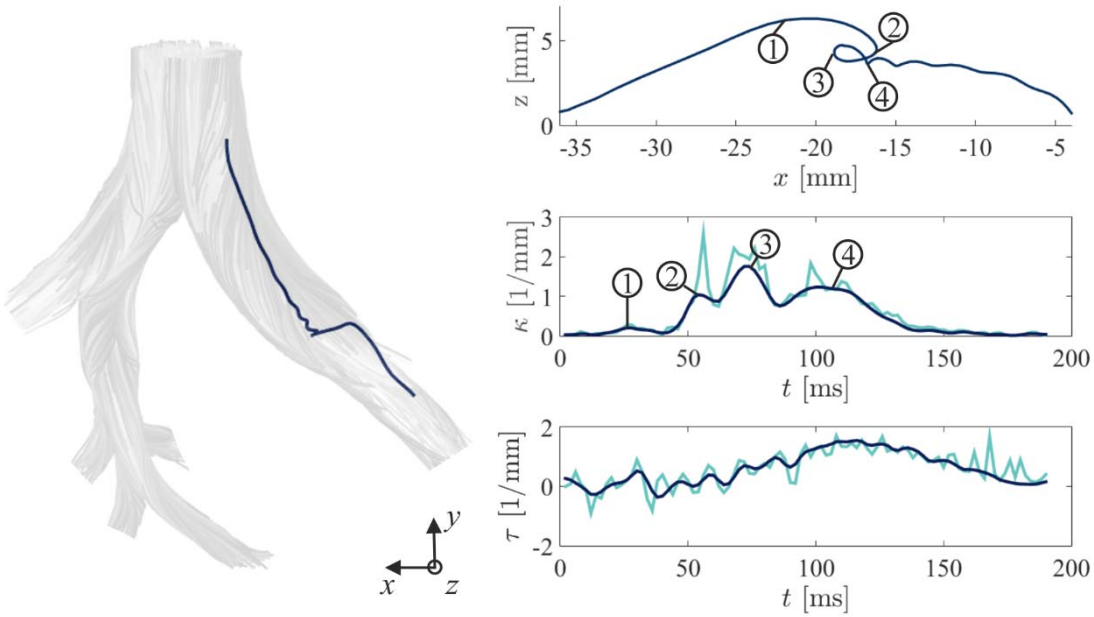


**Fig. 5** Evaluation of a single particle trajectory during peak expiration. Illustration of the particle path position within the reconstructed volume (left), particle path in x-z-plane (right-top), curvature signal: raw, smoothed (right-middle), torsion signal: raw, smoothed (right-bottom).

## Conclusions

The evaluation of curvature and torsion of particle paths inside a realistic model of the human conductive airways, obtained by three-dimensional Particle Tracking Velocimetry (3D-PTV) measurements, have been presented. The investigated model is a generic representation of a human adult lung, covering the airways starting from the trachea down to sixth generation of bifurcation. Using three high-speed cameras and three high-power LEDs we were able to reconstruct the three-dimensional flow field around the main carina at peak inspiration and peak expiration for flow conditions representing breathing under rest conditions ($Re$ = 2000, $\alpha$ = 3.0). After giving a brief description about the used 3D-PTV algorithm, we described the calculation of the curvature and torsion for an idealized helix-curve. We could show that, due to the need of higher derivatives and numerical differentiation, occurring noise has a strong impact on the resulting curvature and torsion signals. However, after applying a robust smoothing algorithm, we were still able to recover the correct values.
The investigation of the local curvature within the whole reconstructed volume revealed areas with high curvature values, caused by particle trajectories under the influence of secondary flow effects. Illustrating the local torsion, we showed, that we can get a measure of the sense of rotation of the Dean-vortices, represented by either positive or negative signs of torsion.
The concrete influence of such a Dean vortex on a single particle could be measured. For such a case we showed the corresponding curvature and torsion. We found local maxima within the curvature signal and an increasing torsion value as the helical particle path get stretched.
To conclude, the curvature and torsion can be used well to highlight important flow properties, especially for flows strongly influenced by secondary motion, as found in the human lung. For the future, we are planning to compare lung models with different geometries and their effect on the corresponding curvature and torsion values to extend the results gained by the here presented study.

## Acknowledgements

The financial support of this study by the Deutsche Forschungsgemeinschaft (grant No. BA 4995/2-1) is gratefully acknowledged.

## References

**Adler, K. and Brücker, C. 2007**: Dynamic flow in a realistic model of the upper human lung airways, *Experiments in Fluids*, 43(2–3), pp. 411–423. doi: 10.1007/s00348-007-0296-0.
**Banko, A. J., Coletti, F., Elkins, C. J. and Eaton, J. K. 2016**: Oscillatory flow in the human airways from the mouth through several bronchial generations, *International Journal of Heat and Fluid Flow*. Elsevier Inc., 61, pp. 45–57. doi: 10.1016/j.ijheatfluidflow.2016.04.006.
**Braun, W., Lillo, F. D. E. and Eckhardt, B. 2006**: Geometry of particle paths in turbulent flows, *Journal of Turbulence*, 7(62). doi: 10.1080/14685240600860923.
**Coletti, A. J. B. F. and Elkins, D. S. C. J. 2015**: Three‐dimensional inspiratory flow in the upper and central human airways, *Experiments in Fluids*. Springer Berlin Heidelberg, 56(6), pp. 1–12. doi: 10.1007/s00348-015-1966-y.
**Dean, W. R. 1928**: Fluid Motion in a Curved Channel, *Proc. R. Soc. Lond. A*, 121(787). doi: https://doi.org/10.1098/rspa.1928.0205.
**Eckmann, D. M. and Grotberg, J. B. 1988**: Oscillatory flow and mass transport in a curved tube, *Journal of Fluid Mechanics*. Cambridge University Press, 188, p. 509. doi: 10.1017/S0022112088000825.
**Fresconi, F. E. and Prasad, A. K. 2007**: Secondary Velocity Fields in the Conducting Airways of the Human Lung, *Journal of Biomechanical Engineering-Transactions of the ASME*, 129(October), pp. 722–732. doi: 10.1115/1.2768374.
**Garcia, D. 2010**: Robust smoothing of gridded data in one and higher dimensions with missing values., *Computational Statistics & Data Analysis*, 54(4), pp. 1167–1178. doi:

10.1016/j.csda.2009.09.020.Robust.
**Horsfield, K., Dart, G., Olson, D. E. and Cumming, G. 1971**: Models of the human bronchial tree, *Journal of Applied Physiology*, 31(2), pp. 207–217.
**Janke, T. and Bauer, K. 2016**: Development of a 3D-PTV algorithm for the investigation of characteristic flow structures in the upper human bronchial tree, in *18th International Symposium on the Application of Laser and Imaging Techniques to Fluid Mechanics*.
**Liberzon, A., Lüthi, B., Holzner, M., Ott, S., Berg, J. and Mann, J. 2012**: On the structure of acceleration in turbulence, *Physica D*. Elsevier B.V., 241(3), pp. 208–215. doi: 10.1016/j.physd.2011.07.008.
**Malik, N. A. and Papantoniou, D. A. 1993**: Particle tracking velocimetry in three-dimensional flows Part II : Particle tracking, *Experiments in Fluids*, 294, pp. 279–294.
**Mass, H. G., Gruen, A. and Papantoniou, D. 1993**: Particle tracking velocimetry in three-dimensional flows Part I Photogrammetric determination of particle coordinates, *Experiments in Fluids*, 146, pp. 133–146.
**Schanz, D., Schröder, A., Gesemann, S., Michaelis, D. and Wieneke, B. 2013**: ' Shake The Box ': A highly efficient and accurate Tomographic Particle Tracking Velocimetry ( TOMO-PTV ) method using prediction of particle positions, in *10th International Symposium on Particle Image Velocimetry*.
**Schröder, F., Bordin, S., Härtel, S., Washausen, M. and Schröder, W. 2012**: Comparison of steady and unsteady exhalation using multiplane-stereo PIV, in *16th International Symposium on the Applications of Laser Techniques to Fluid Mechanics*.
**Schroter, R. C. and Sudlow, M. F. 1969**: Flow patterns in models of the human bronchial airways, *Respiration Physiology*, 7, pp. 341–355.
**Weibel, E. R. 1963**: Morphometry of the human lung. Springer-Verlag.
**Wieneke, B. 2013**: Iterative reconstruction of volumetric particle distribution, *Measurement Science and Technology*, 24. doi: 10.1088/0957-0233/24/2/024008.
**Xu, H., Ouellette, N. T. and Bodenschatz, E. 2007**: Curvature of Lagrangian Trajectories in Turbulence, *Physical Review Letters*, 98(February), pp. 1–4. doi: 10.1103/PhysRevLett.98.050201.